J|A|C|S
ARTICLES
Published on Web 11/27/2002

Coverage Effects and the Nature of the Metal−Sulfur Bond in S/Au(111): High-Resolution Photoemission and Density-Functional Studies

José A. Rodriguez,*,† Joseph Dvorak,† Tomas Jirsak,† Gang Liu,† Jan Hrbek,† Yosslen Aray,‡,§ and Carlos González§

Contribution from the Department of Chemistry, Brookhaven National Laboratory, Upton, New York 11953, Centro de Química, Instituto Venezolano de Investigaciones Cientificas (IVIC), Apartado 21827, Caracas 1020 A, Venezuela, and Physical and Chemical Properties Division, National Institute of Standard and Technologies (NIST), Gaithersburg, Maryland 20899

Received July 22, 2002; E-mail: rodrigez@bnl.gov

Abstract: The bonding of sulfur to surfaces of gold is an important subject in several areas of chemistry, physics, and materials science. Synchrotron-based high-resolution photoemission and first-principles density-functional (DF) slab calculations were used to study the interaction of sulfur with a well-defined Au(111) surface and polycrystalline gold. Our experimental and theoretical results show a complex behavior for the sulfur/Au(111) interface as a function of coverage and temperature. At small sulfur coverages, the adsorption of S on fcc hollow sites of the gold substrate is energetically more favorable than adsorption on bridge or a-top sites. Under these conditions, S behaves as a weak electron acceptor but substantially reduces the density-of-states that gold exhibits near the Fermi edge. As the sulfur coverage increases, there is a weakening of the Au−S bonds (with a simultaneous reduction in the Au → S charge transfer and a modification in the S sp hybridization) that facilitates changes in adsorption site and eventually leads to S−S bonding. At sulfur coverages above 0.4 ML, S_2 and not atomic S is the more stable species on the gold surface. Formation of S_n ($n > 2$) species occurs at sulfur coverages higher than a monolayer. Very similar trends were observed for the adsorption of sulfur on polycrystalline surfaces of gold. The S atoms bonded to Au(111) display a unique mobility/reactivity not seen on surfaces of early or late transition metals.

I. Introduction

In general, the bonding of sulfur to surfaces of metals is an important topic in catalysis,[1−3] electrochemistry,[4−6] interfacial physics,[7,8] and materials science.[9−12] The reaction of sulfur with a metal can produce adsorbed sulfur species or sulfide compounds, dramatically changing the chemical properties of the metal element.[1−3,13] In the chemical and petrochemical industries, millions of dollars are lost every year due to the negative effects of sulfur poisoning on the activity and selectivity of supported metal catalysts.[2,3] Sulfur-containing molecules are frequently found as impurities in petroleum-derived chemical feedstocks and synthesis gas.[2,3] These sulfur-containing molecules decompose, and sulfur species are deposited on metal catalysts used for the reformation or transformation of hydrocarbons, the hydrogenation of olefins, the synthesis of methanol, the oxidation of CO, the reduction of NO, the water-gas shift reaction, etc.[2,3] On metal catalysts, sulfur poisoning is a complex phenomenon that can arise from blocking the access of reactants or intermediates to active sites (i.e., deactivation by steric effects) or from a direct modification of the chemical properties of the

* To whom correspondence should be addressed. Fax: 631-344-5815.
† Brookhaven National Laboratory.
‡ IVIC.
§ National Institute of Standard and Technologies.

(1) Rodriguez, J. A.; Hrbek, J. *Acc. Chem. Res.* **1999**, *32*, 719.
(2) Bartholomew, C. H.; Agrawal, P. K.; Katzer, J. R. *Adv. Catal.* **1982**, *31*, 135.
(3) (a) Thomas, J. M.; Thomas, W. J. *Principles and Practice of Heterogeneous Catalysis*; VCH: New York, 1997. (b) Somorjai, G. A. *Introduction to Surface Chemistry and Catalysis*; Wiley: New York, 1994. (c) Hoffmann, R. *Solids and Surfaces: A Chemist's View of Bonding in Extended Structures*; VCH: New York, 1988.
(4) (a) Martin, H.; Vericat, C.; Andreasen, G.; Hernández-Creus, A.; Vela, M. E.; Salvarezza, R. C. *Langmuir* **2001**, *17*, 2334. (b) Vericat, C.; Vela, M. E.; Andreasen, G.; Salvarezza, R. C.; Vázquez, L.; Martin-Gago, J. A. *Langmuir* **2001**, *17*, 4919.
(5) (a) Tong, Y. Y.; Rice, C.; Wieckowski, A.; Oldfield, E. *J. Am. Chem. Soc.* **2000**, *122*, 11921. (b) Sung, Y. E.; Chrzanowski, W.; Zolfaghari, A.; Jerkiewicz, G.; Wieckowski, A. *J. Am. Chem. Soc.* **1997**, *119*, 194.
(6) Kolb, D. M. In *Advances in Electrochemistry and Electrochemical Engineering*; Gerisher, H., Tobias, C. W., Eds.; Interscience: New York, 1978.
(7) Yang, Z.; Wu, R.; Rodriguez, J. A. *Phys. Rev. B* **2002**, *65*, 155409.
(8) (a) Demuth, J. E.; Jepsen, D. W.; Marcus, P. M. *Phys. Rev. Lett.* **1973**, *31*, 540. (a) Brennan, S.; Stöhr, J.; Jaeger, R. *Phys. Rev. B* **1981**, *24*, 4871. (c) Polčik, M.; Wilde, L.; Haase, J. *Phys. Rev. B* **1998**, *57*, 1868.
(9) Ulman, A. *Chem. Rev.* **1996**, *96*, 1533.
(10) (a) Flis, J., Ed. *Corrosion of Metals and Hydrogen-Related Phenomena*; Elsevier: Amsterdam, 1991. (b) Marcus, P.; Oudar, J. In *Passivity of Metals and Semiconductors*; Froment, M., Ed.; Elsevier: Amsterdam, 1983.
(11) (a) Poirier, G. E.; Tarlov, M. J. *J. Phys. Chem.* **1995**, *99*, 10966. (b) Poirier, G. E. *Chem. Rev.* **1997**, *97*, 1117. (c) Fenter, P.; Eberhardt, A.; Eisenberger, P. *Science* **1994**, *266*, 1216.
(12) (a) Camillone, N.; Chidsey, C. E. D.; Liu, G.-Y.; Scoles, G. *J. Chem. Phys.* **1993**, *98*, 3503. (b) Camillone, N.; Chidsey, C. E. D.; Eisenberger, P.; Fenter, P.; Li, J.; Liang, K. S.; Liu, G.-Y.; Scoles, G. *J. Chem. Phys.* **1993**, *99*, 744.
(13) (a) Weisser, O.; Landa, S. *Sulfide Catalysts: Their Properties and Applications*; Pergamon: Oxford, 1973. (b) Aray, Y.; Rodriguez, J.; Vega, D.; Rodriguez-Arias, E. N. *Angew. Chem., Int. Ed.* **2000**, *39*, 3810.

 10.1021/ja021007e CCC: $25.00

active sites (i.e., deactivation by electronic effects).[1−3,14] To minimize the negative effects of sulfur poisoning, one needs a fundamental and general understanding of metal−sulfur interactions.[1−3,7,14,15] Recently, gold has become the subject of a lot of attention due to its unusual catalytic properties when dispersed on some oxide supports (TiO_2, CrO_x, MnO_x, Fe_2O_3, Al_2O_3, MgO).[16−21] Several models have been proposed for explaining the interesting behavior of supported gold,[16−20] and in many situations the special catalytic properties of this system or bulk metallic Au disappear as a consequence of sulfur poisoning.[2,3,21]

Gold surfaces are also used as models to examine the adsorption of sulfur in electrochemical studies (the ability of sulfur to modify the properties of metal electrodes is broadly recognized)[4,7] and as templates for growing self-assembled monolayers (SAMs) of thiols and related organosulfur molecules.[9,11,12] These compounds undergo S−H bond cleavage and bind to the gold substrate via the S-end.[9,12] Given the wealth of potential technological applications (lithography, lubrication, development of sensors, corrosion inhibition, catalysis, molecular recognition, etc.), the interest in the underlying chemistry and physics of SAMs has been steadily growing during the past decade.[9,11b,22−32] Independent of the type of organic chain present, basic issues about the nature of the sulfur/gold interface are still open.[9,12,22−32] For alkylthiols (RS) on Au(111), studies with various experimental techniques point to different adsorption sites for S, some of them contrary to chemical intuition.[11,12,23,24,28,33] An identical situation is found in theoretical works.[22,24,27,29,30,32] For example, ab initio cluster calculations for CH_3S on Au(111) predict bonding on hcp hollow sites.[24] In contrast, density-functional (DF) slab calculations give either the bridge[29,30,32] or the hollow fcc[22,27] as the most stable adsorption site for CH_3S on Au(111). A change in adsorption site with coverage has been proposed by some authors[9,11b] and rejected by others.[27,30] Another important point of controversy is the possible formation of S−S bonds in the sulfur/gold interface.[11c,12,23a,24,28a,33,34] According to the "standard model", alkylthiols occupy three-fold hollow sites of the Au(111) substrate with S−S spacings of ∼5 Å.[12a,23a,24,33] On the other hand, in the "sulfur-pairing model", alkylthiols form sulfur-headgroup dimers with S−S spacings of 2.2 Å.[11c,12b,28a,34] For all of these reasons, it is important to study the bonding in a sulfur/gold interface and how this "simple" system behaves as a function of adsorbate coverage and temperature.

In this article, we use synchrotron-based high-resolution photoemission, thermal desorption mass spectroscopy (TDS), and first-principles DF calculations to carry out a systematic study of the interaction of sulfur with Au(111) and polycrystalline gold. High-resolution photoemission is very sensitive to changes in the adsorption site of sulfur on metals and to the formation of S−S bonds.[1,35−37] Following the approach of previous theoretical studies,[22,24,27,29,30,32] we perform DF calculations using pseudopotentials to describe the core electrons of Au and S, but in this work we also carry out first-principles calculations that include *all* of the electrons in the S/Au system. A series of exchange-correlation functionals based on the generalized-gradient approximation (GGA) are utilized: Perdew−Wang (PW91),[38] Purdue−Burke−Ernzerhof (PBE),[39] and a revised version of this functional (RPBE) developed to provide better values of chemisorption energies.[40] In this way, we obtain a robust theoretical description of the sulfur/Au(111) interface. Our experimental and theoretical results show that sulfur atoms bonded to Au(111) have a unique mobility (not seen on surfaces of other transition metals) that allows them the facile change of adsorption site with coverage and the formation of S_n aggregates.

II. Experimental and Theoretical Methods

II.1. Photoemission and Thermal Desorption Experiments. The photoemission experiments for the adsorption of sulfur on Au(111) and polycrystalline surfaces of gold were performed in a standard ultrahigh vacuum chamber (base pressure $\sim 6 \times 10^{-10}$ Torr) that is part of the U7A beamline of the National Synchrotron Light Source (NSLS) at Brookhaven National Laboratory.[41] This ultrahigh vacuum (UHV) chamber contains a hemispherical electron energy analyzer with multichannel detection, instrumentation for low-energy electron diffraction (LEED), a quadrupole mass spectrometer, and a dual anode Mg/Al Kα X-ray source. The S 2p, Au 4f, and valence spectra were taken using a photon energy of 380 or 260 eV. The binding energy scale of the photoemission spectra was calibrated by the position of the Fermi edge.[41] The energy resolution in the photoemission experiments was 0.3−0.4 eV. Mounting of the Au(111) sample in the UHV chamber was done following the procedure described in ref 42. In short, the gold crystal was held by one 0.5 mm diameter tantalum wire wrapped along a groove machined in the edge of the crystal. The sample could

(14) (a) Goodman, D. W. *Appl. Surf. Sci.* **1984**, *19*, 1. (b) Campbell, C. T. *Adv. Catal.* **1989**, *36*, 1. (c) Rodriguez, J. A.; Goodman, W. D. *Surf. Sci. Rep.* **1991**, *14*, 1.
(15) Oudar, J., Wise, H., Eds.; *Deactivation and Poisoning of Catalysts*; Marcel Dekker: New York, 1983.
(16) Haruta, M. *Catal. Today* **1997**, *36*, 153.
(17) Valden, M.; Lai, X.; Goodman, D. W. *Science* **1998**, *281*, 1647.
(18) (a) Rodriguez, J. A.; Chaturvedi, S.; Kuhn, M.; van Ek, J.; Diebold, U.; Robbert, P. S.; Geisler, H.; Ventrice, C. A. *J. Chem. Phys.* **1997**, *107*, 9146. (b) Rodriguez, J. A.; Liu, G.; Jirsak, T.; Hrbek, J.; Chang, Z.; Dvorak, J.; Maiti, A. *J. Am. Chem. Soc.* **2002**, *124*, 5242.
(19) (a) Bondzie, V. A.; Parker, S. C.; Campbell, C. T. *J. Vac. Sci. Technol., A* **1999**, *17*, 1717. (b) Bondzie, V. A.; Parker, S. C.; Campbell, C. T. *Catal. Lett.* **1999**, *63*, 143. (c) Ajo, H. M.; Bonzie, V. A.; Campbell, C. T. *Catal. Lett.* **2002**, *78*, 359.
(20) Sanchez, A.; Abbet, S.; Heiz, U.; Schneider, W. D.; Hakkinen, H.; Barnett, R. N.; Landman, U. *J. Phys. Chem. A* **1999**, *103*, 9573.
(21) Bond, G. C.; Thompson, D. T. *Catal. Rev.−Sci. Eng.* **1999**, *41*, 319.
(22) Gronbeck, H.; Curioni, A.; Andreoni, W. *J. Am. Chem. Soc.* **2000**, *122*, 3839.
(23) (a) Dubois, L. H.; Zegarski, B. R.; Nuzzo, R. G. *J. Chem. Phys.* **1993**, *98*, 678. (b) Nuzzo, R. G.; Allara, D. L. *J. Am. Chem. Soc.* **1983**, *105*, 4481.
(24) (a) Sellers, H.; Ulman, A.; Shnidman, Y.; Eilers, J. E. *J. Am. Chem. Soc.* **1993**, *115*, 9389. (b) Beardmore, K. M.; Kress, J. D.; Gronbech-Jensen, N.; Bishop, A. R. *Chem. Phys. Lett.* **1998**, *40*, 286.
(25) Hakkinen, H.; Barnett, R. N.; Landman, U. *Phys. Rev. Lett.* **1999**, *16*, 3264.
(26) Kruger, D.; Fuchs, H.; Rousseau, R.; Marx, D.; Parinello, M. *J. Chem. Phys.* **2001**, *115*, 4776.
(27) Yourdshahyan, Y.; Zhang, H. K.; Rappe, A. M. *Phys. Rev. B* **2001**, *63*, R081405.
(28) (a) Fenter, P.; Schreiber, F.; Berman, L.; Scoles, G.; Eisenberger, P.; Bedzyk, M. J. *Surf. Sci.* **1998**, *412/413*, 213. (b) Kluth, G. J.; Carraro, C.; Maoudian, R. *Phys. Rev. B* **1999**, *59*, R10449.
(29) Hayashi, T.; Morikawa, Y.; Nozoye, H. *J. Chem. Phys.* **2001**, *114*, 7615.
(30) Vargas, M. C.; Giannozzi, P.; Selloni, A.; Scoles, G. *J. Phys. Chem. B* **2001**, *105*, 9509.
(31) Akinaga, Y.; Nakajima, T.; Hirao, K. *J. Chem. Phys.* **2001**, *114*, 8555.
(32) Gottschalck, J.; Hammer, B. *J. Chem. Phys.* **2002**, *116*, 784.
(33) (a) Porter, M. D.; Bright, T. B.; Allara, D. L.; Chidsey, C. E. D. *J. Am. Chem. Soc.* **1987**, *109*, 3559. (b) Arce, F. T.; Vela, M. E.; Salvarezza, R. C.; Arvia, A. J. *Langmuir* **1998**, *14*, 7203.
(34) Gerdy, J. J.; Goddard, W. A. *J. Am. Chem. Soc.* **1996**, *118*, 3223.
(35) Mullins, D. R.; Lyman, P. F.; Overbury, S. H. *Surf. Sci.* **1992**, *277*, 64 and references therein.
(36) (a) Rodriguez, J. A.; Chaturvedi, S.; Jirsak, T. *Chem. Phys. Lett.* **1998**, *296*, 421. (b) Rodriguez, J. A.; Hrbek, J.; Kuhn, M.; Chaturvedi, S.; Maiti, A. *J. Chem. Phys.* **2000**, *113*, 11284.
(37) Hrbek, J.; Li, S. Y.; Rodriguez, J. A.; van Campen, D. G.; Huang, H. H.; Xu, G.-Q. *Chem. Phys. Lett.* **1997**, *267*, 65.
(38) White, J. A.; Bird, D. M. *Phys. Rev. B* **1994**, *50*, 4954.
(39) Perdew, J. P.; Burke, K.; Ernzerhof, M. *Phys. Rev. Lett.* **1996**, *77*, 3865.
(40) Hammer, B.; Hansen, L. B.; Norkskov, J. K. *Phys. Rev. B* **1999**, *59*, 7413.
(41) (a) Rodriguez, J. A.; Jirsak, T.; Chaturvedi, S.; Hrbek, J. A. *J. Am. Chem. Soc.* **1998**, *120*, 11149. (b) Jirsak, T.; Rodriguez, J. A.; Hrbek, J. *Surf. Sci.* **1999**, *426*, 319.

be cooled to as low as 100 K by thermal contact with a liquid nitrogen reservoir and resistively heated to 1200 K. The temperature was monitored by a type C thermocouple inserted in a hole at the sample edge. The Au(111) surface was cleaned by repeated cycles of 1 keV Ne^+ ion bombardment followed by heating at 900 K until no impurities were detected by photoemission. Photoemission experiments were also carried out for the adsorption of sulfur on polycrystalline surfaces of gold. These rough surfaces were generated by vapor depositing multilayers of gold on a Mo(110) substrate as described in previous work.[43]

The thermal desorption experiments for sulfur/Au(111) were done in a second UHV chamber (with a base pressure of $\sim 5 \times 10^{-10}$ Torr) equipped with a hemispherical electron energy analyzer with single channel detection, a dual X-ray source, and a residual gas analyzer (SRS-RGA). The residual gas analyzer was surrounded by a stainless steel jacket with a 10-mm aperture for the TDS measurements. The crystal was positioned 1−2 mm away from the aperture to prevent contributions of TDS signals from surfaces other than the sample. All of the TDS spectra were collected at a heating rate of 2 K/s. The sample was mounted as described above for the photoemission measurements.

In both UHV chambers, S_2 gas was generated in situ from decomposition of silver sulfide in a solid-state electrochemical cell, $Pt/Ag/AgI/Ag_2S/Pt$.[37,44] The dosing of S_2 was performed at sample temperatures of 100 or 300 K.

II.2. First-Principles Density Functional Calculations. We carried out self-consistent first-principles calculations within the Kohn−Sham density-functional (DF) theory using the CASTEP code.[45] In this code, the wave functions of valence electrons are expanded in a plane wave basis set with k-vectors within a specified energy cutoff E_{cut}. Tightly bound core electrons are represented by nonlocal ultrasoft pseudopotentials.[46] Brillouin Zone integration is approximated by a sum over special k-points chosen using the Monkhorst−Pack scheme.[47] The exchange-correlation contribution to the total electronic energy is treated in a generalized-gradient corrected (GGA) extension of the local density approximation (LDA) using the PW91,[38] PBE,[39] or RPBE[40] functionals. In all of the calculations, the kinetic energy cutoff E_{cut} (400 eV) and the density of the Monkhorst−Pack k-point mesh {$8 \times 8 \times 1$ grid for the smallest (1×1) cells, reduced to a $8 \times 5 \times 1$ grid for the largest (2×2) cells} were chosen high enough to ensure convergence of the computed structures and energetics. For each optimized structure, the partial charges on the atoms were estimated by projecting the occupied one-electron eigenstates onto a localized basis set with a subsequent Mulliken population analysis.[48,49] Mulliken charges have well-known limitations,[50] but experience has shown that they are nevertheless useful as a qualitative tool.

We also performed full-electron first-principles calculations for the S/Au(111) system using the WIEN-97 program,[51] which contains a full-potential linearized augmented plane-wave (FLAPW) method[51−54] that is considered to be among the most accurate methods for performing electronic structure calculations for crystals. The unit cell is divided into a region containing nonoverlapping atomic spheres (centered at the atomic sites) called muffin-tins, MT, and an interstitial region, IT. In the two types of regions, different basis sets are used: a linear combination of radial functions times spherical harmonics inside MT and a plane wave expansion in IT. Inside the spheres, the potential and charge density were expanded in lattice harmonics up to $l = 12$. A basis set size of about 500 augmented plane-waves per atom with cutoffs $R_{MT}K_{max} = 9.0$ was used. Fifty-six points over the Brillouin Zone and a quadratic tetrahedron method were chosen for k-space numerical integration. The full-electron calculations were done using the PBE exchange-correlation functional.[39]

Because all of the DF calculations were performed at the GGA level, one can expect reasonable predictions for the bonding energies of sulfur on different adsorption sites of Au(111).[39,40] In any case, in this work our main interest is in qualitative trends in the energetics, and not in absolute values. The adsorption energy (AE) of sulfur was calculated through the expression: AE = −{S/Au(111) − Au(111) − S(atoms in cell)}. Following the usual convention, positive values of AE denote an exothermic adsorption process. Spin polarization was used for calculating S in the gas phase.[32] After several tests, we found no need for spin polarization in calculations involving S/Au(111).[11]

III. Results and Discussion

III.1. Adsorption of Sulfur on Au(111), Polycrystalline Gold, and Other Metals. Figure 1 shows S 2p photoemission data for the adsorption of sulfur on Au(111) at 300 K. Even for small doses of S_2 (two spectra at the bottom, above background trace), the spectra have to be curve-fitted[37,41] by a set of three doublets with $2p_{3/2}$ components at ~160.8 (dominant doublet), 161.6, and 163.4 eV (very weak doublet). Comparison to previous studies[37,41] indicates that the two doublets toward lower binding energy correspond to sulfur atoms in different adsorption sites. In a separate set of experiments, we found that after annealing similar systems to 500 K, the doublet with the $2p_{3/2}$ component near 160.8 eV gained intensity with respect to the other two. This doublet was by far the main S 2p signal for sulfur/Au(111) surfaces that exhibited a $(\sqrt{3} \times \sqrt{3})R30°$ LEED pattern.[4] It can be assigned to S atoms bonded to three-fold hollow sites of the Au(111) surface; see ref 4b and discussion below. The $(\sqrt{3} \times \sqrt{3})R30°$ LEED pattern disappeared as the sulfur coverage increased (>0.35 ML) and the S 2p features above 163 eV rapidly gained intensity, being dominant when the surface was saturated with a chemisorbed layer of the adsorbate at 300 K. These high-binding energy S 2p features denote the presence of S_n aggregates ($n = 2$) on the metal surface.[36,37] The TDS and theoretical results described below indicate that they mainly originate from adsorbed S_2. Strong evidence for the existence of S_n ($n > 2$) was found when dosing sulfur at 100 K and depositing more than a monolayer of the adsorbate on the surface. The graph in Figure 1 shows in detail the evolution of the different sulfur species as a function of coverage upon dosing at 300 K (without subsequent annealing to high temperatures). Initially, at small sulfur coverages, S atoms on hollow sites were the main surface species. Yet as the dosing of sulfur increased above 0.33 ML (roughly judged by the disappearance of the $(\sqrt{3} \times \sqrt{3})R30°$ LEED pattern), the S atoms recombined (clear decrease in corresponding S 2p

(42) (a) Rodriguez, J. A.; Dvorak, J.; Jirsak, T.; Hrbek, J. *Surf. Sci.* **2001**, *490*, 315. (b) Liu, G.; Rodriguez, J. A.; Dvorak, J.; Hrbek, J.; Jirsak, T. *Surf. Sci.* **2002**, *505*, 295.
(43) Rodriguez, J. A.; Kuhn, M. *Surf. Sci.* **1995**, *330*, L657.
(44) Heegemann, W.; Meister, K. H.; Bechtold, E.; Hayek, K. *Surf. Sci.* **1975**, *49*, 161.
(45) (a) Payne, M. C.; Allan, D. C.; Arias, T. A.; Johannopoulus, J. D. *Rev. Mod. Phys.* **1992**, *64*, 1045. (b) Milman, V.; Winkler, B.; White, J. A.; Pickard, C. J.; Payne, M. C.; Akhmatskaya, E. V.; Nobes, R. H. *Int. J. Quantum Chem.* **2000**, *77*, 895.
(46) Vanderbilt, D. *Phys. Rev. B* **1990**, *41*, 7892.
(47) Monkhorst, H. J.; Pack, J. D. *Phys. Rev. B* **1976**, *13*, 5188.
(48) Segall, M. D.; Pickard, C. J.; Shah, R.; Payne, M. C. *Phys. Rev. B* **1996**, *54*, 16317.
(49) Segall, M. D.; Pickard, C. J.; Shah, R.; Payne, M. C. *Mol. Phys.* **1996**, *89*, 571.
(50) (a) Szabo, A.; Ostlund, N. S. *Modern Quantum Chemistry*; McGraw-Hill: New York, 1989. (b) Wiberg, K. B.; Rablen, P. R. *J. Comput. Chem.* **1993**, *14*, 1504.
(51) Blaha, P.; Schwarz, K.; Luitz, J. *WIEN 97*, Vienna University of Technology, 1997. (Improved and updated Unix version of the original copyrighted WIEN-code, which was published by Blaha, P.; Schwarz, K.; Sorantin, P.; Trickey, S. B. *Comput. Phys. Commun.* **1990**, *59*, 399.
(52) Singh, D. J. *Planewaves, Pseudopotentials, and the LAPW Method*; Kluwer Academic: Boston, 1994.
(53) Petersen, M.; Wagner, F.; Hufnagel, L.; Scheffler, M.; Blaha, P.; Schwarz, K. *Comput. Phys. Commun.* **2000**, *126*, 294.
(54) Schwarz, K.; Ambrosch-Draxt, C.; Blaha, P. *Phys. Rev. B* **1990**, *42*, 2051.

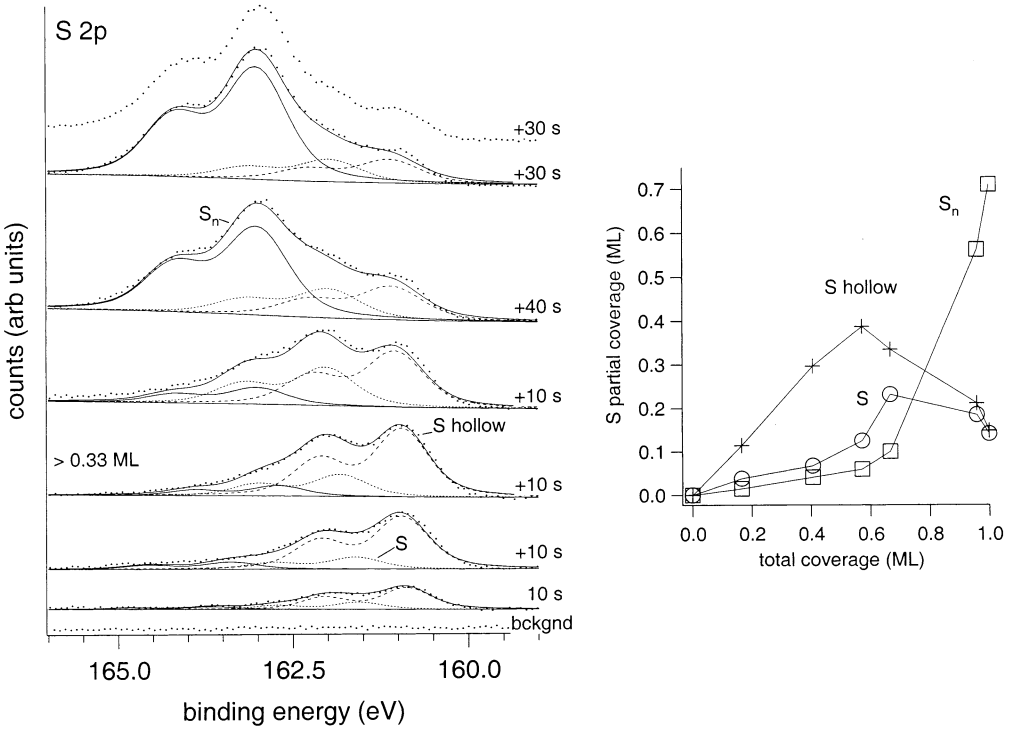

Figure 1. Left: S 2p spectra for the adsorption of sulfur on Au(111) at 300 K. Right: Partial coverage for the different sulfur species as a function of total coverage. The partial coverages were derived from the area under the corresponding S 2p doublets.

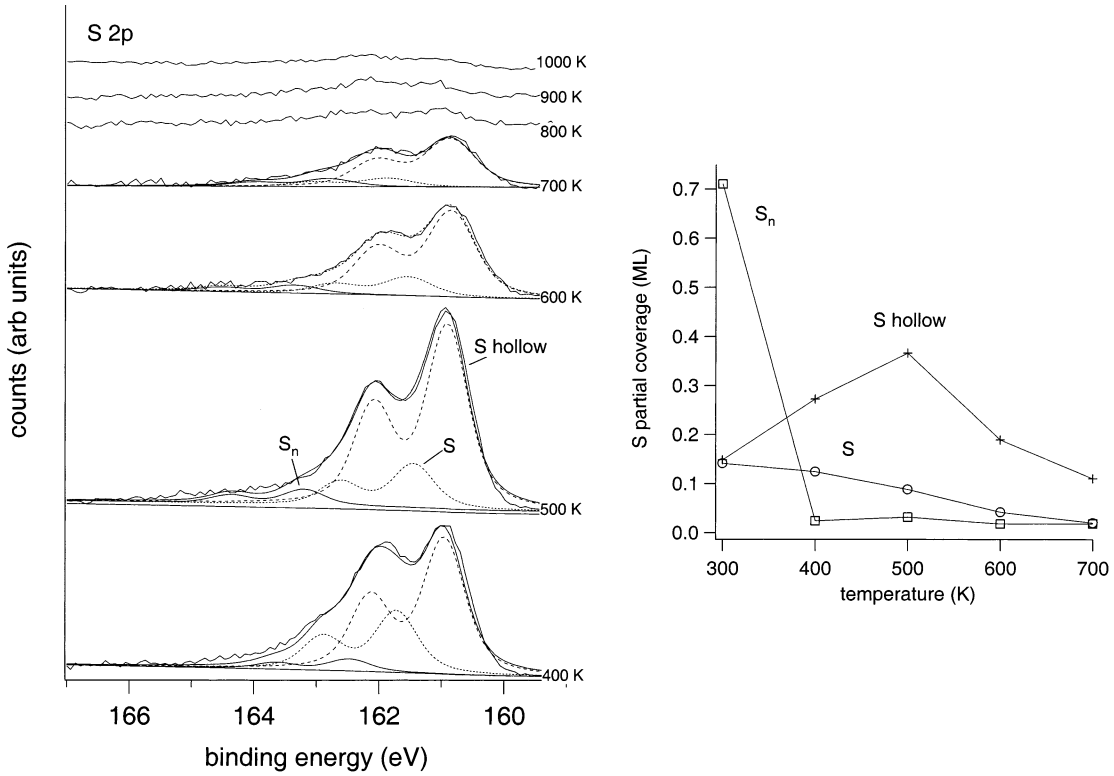

Figure 2. Left: S 2p spectra acquired after heating a surface initially saturated with chemisorbed sulfur at 300 K. Right: Partial coverage for the different sulfur species as a function of temperature. The partial coverages were derived from the area under the curve-fitted S 2p doublets. The initial point (300 K) corresponds to the last spectrum in Figure 1.

signal), and S_n aggregates became dominant on the surface. *Thus, sulfur atoms bonded to Au(111) at room temperature are reactive enough to form S−S bonds at moderate and high coverages.* This is consistent with a reduction in the strength of the Au−S bond as the adsorbate coverage increases.

Figure 2 shows S 2p data acquired after heating a saturated layer of chemisorbed sulfur (last spectrum in Figure 1) from 300 to 1000 K. Most of the S 2p signal for S_n disappears below 400 K. As the overall coverage of sulfur decreases, the amount of adsorbed S_n species diminishes, while there is an increase in

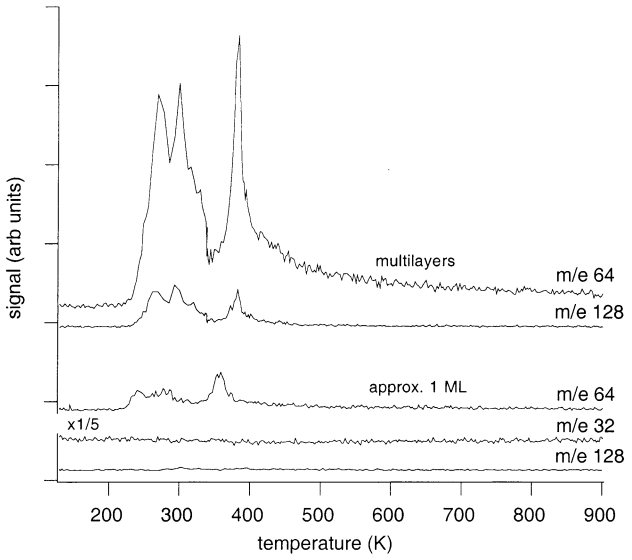

Figure 3. Bottom traces: Thermal desorption data ($m/e = 32$, 64, or 128) for ~1 layer of chemisorbed sulfur on Au(111). Top traces: Thermal desorption data ($m/e = 64$ and 128) for a sulfur multilayer. The dosing of sulfur was carried out at 100 K. Heating rate = 2 K/s.

the coverage of atomic S bonded to hollow sites of Au(111). As seen in the adsorption experiments of Figure 1, *here there is also a clear indication for a large variation in the strength of the Au−S and S−S bonds with coverage.* Furthermore, it is likely that S atoms bonded to Au(111) have a relatively large mobility, which allows them the facile change of adsorption site and the formation of S_n aggregates when θ_S varies.

The three curves at the bottom of Figure 3 show TDS data for ~1 layer of chemisorbed sulfur on Au(111). The two curves at the top display the corresponding data for a multilayer of sulfur obtained by dosing sulfur at 100 K.[37] In the case of the multilayer, there is coexistence of molecular species such as S_2, S_4, S_6, and S_8,[37] and in our TDS experiments we observed evolution of masses 64 (S_2), 96 (S_3, not shown in figure), and 128 (S_4) from 280 to 450 K. For the monolayer, only desorption of mass 64 (S_2, 300−450 K) was seen. At 500 K, S was still present on the gold surface (Figure 2), but its S 2p intensity disappeared in a wide range of temperature (500−800 K) without yielding a significant signal for S or S_2 in TDS.

Photoemission data for the adsorption of sulfur on a rough surface of gold are shown in Figure 4. This polycrystalline surface of gold was prepared by vapor-depositing a thick film of Au on a Mo(110) crystal at 300 K[43] and did not show a LEED pattern. At small doses of sulfur, one sees a doublet in the S 2p region that indicates the presence of atomic S bonded to hollow sites of the Au surface (see above). As the sulfur coverage increases, the S 2p spectra become complex, and a set of three or four doublets (not shown) is necessary to curve-fit them. After a large dose of sulfur at 300 K (saturated monolayer), features for S and S_n are clear in the S 2p spectrum. A comparison to the corresponding spectrum in Figure 1 for sulfur/Au(111) shows that on the rough film the relative amount of atomic S is larger than on the nearly flat surface. Yet in both systems, changes in the S/S_n ratio indicate a variation in the relative strength of the Au−S and S−S interactions with sulfur coverage. This seems to be a general property of sulfur/gold interfaces, because an identical phenomenon has been observed

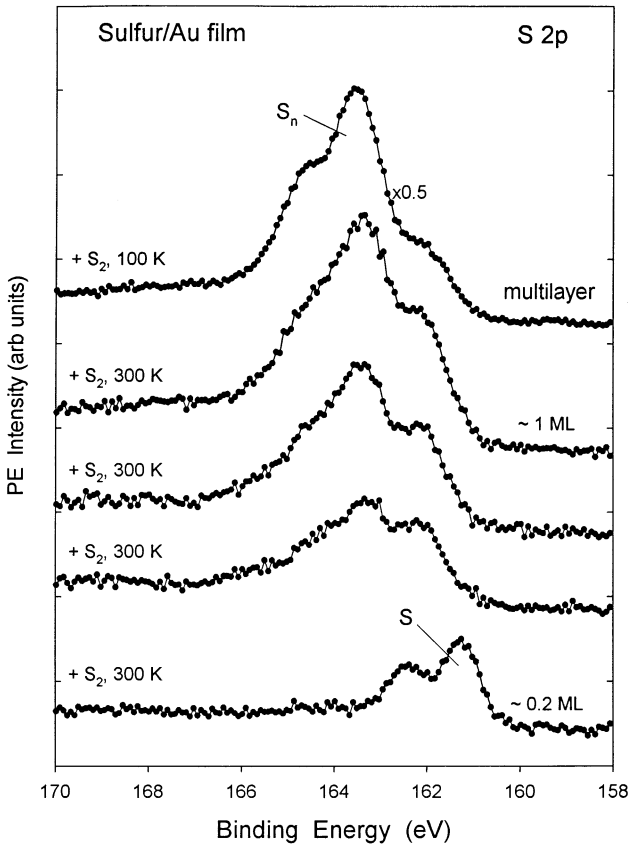

Figure 4. S 2p photoemission spectra for the adsorption of sulfur on a polycrystalline surface of gold. Initially, the surface was saturated with chemisorbed sulfur at 300 K. In the final step, the sample was cooled to 100 K, and a multilayer of sulfur was vapor-deposited.

with scanning tunneling microscopy (STM) during the electroadsorption of sulfur on gold from $NaOH/Na_2S$ solutions.[4b]

It is worthwhile to compare the behavior of sulfur on Au(111) and well-defined surfaces of other transition metals. Figure 5 summarizes the results of photoemission studies for the sulfur/Pt(111) system at 300 K.[36b,55] At a small sulfur coverage (0.15 ML), only a doublet is seen in the S 2p region arising from S atoms bonded to fcc-hollow sites of the Pt(111) surface.[56] As the coverage of sulfur increases on the surface (>0.3 ML), new features appear in the S 2p spectra.[36b,55] The spectrum for 0.93 ML of sulfur contains contributions from two different types of sulfur species: atomic S ("a" in Figure 5) and S_n aggregates ("b" in Figure 5). The situation is somewhat similar to that seen in Figure 1 for sulfur/Au(111), but there are important differences. On Pt(111), there is no signal for S_n species at small coverages (<0.3 ML), and a $nS \rightarrow S_n$ transformation does not occur when the sulfur coverage increases (panel in bottom-right of Figure 5). Thus, the S atoms bonded to Au(111) have a higher mobility/reactivity than those bonded to Pt(111). An even larger difference in behavior is found when comparing to S atoms bonded to early-transition metals.[35,41b] Figure 6 displays S 2p spectra acquired after adsorbing sulfur on Mo(110) at 300 K. Independent of adsorbate coverage, the dominant species on the surface is atomic S. The same result is found on W(100).[35]

(55) (a) Rodriguez, J. A.; Kuhn, M.; Hrbek, J. *Chem. Phys. Lett.* **1996**, *251*, 13. (b) Rodriguez, J. A.; Kuhn, M.; Rodriguez, J. A. *J. Phys. Chem.* **1996**, *100*, 15494.

(56) Kayek, K.; Glassl, H.; Gutmann, A.; Leonhard, H.; Prutton, M.; Tear, S. P.; Welton-Cook, M. R. *Surf. Sci.* **1985**, *152/153*, 419.

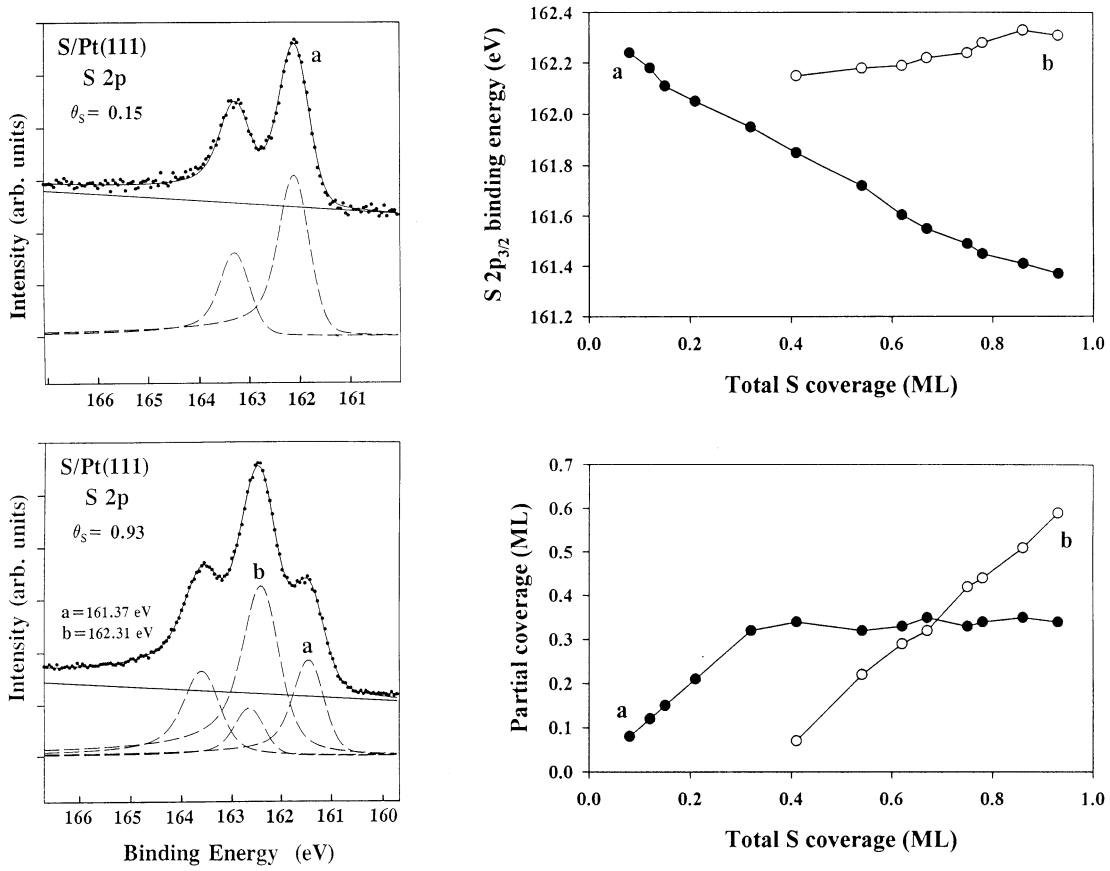

Figure 5. Left side: S 2p photoemission spectra for the adsorption of 0.15 and 0.93 ML of sulfur on Pt(111).[55] Right side: Variation of the S $2p_{3/2}$ binding energy and partial coverage of the "a" (atomic S) and "b" species (S_n aggregates) with total sulfur coverage.[36b,55] The sulfur was deposited using a S_2 source, and the coverage is reported with respect to the atomic density of a Pt(111) surface.

An inverse correlation can be observed between the strength of the metal−sulfur bonds (Mo ≈ W ≫ Pt > Au[35,36b,41b]) and the formation of S−S bonds within the sulfur overlayer (Mo ≈ W ≪ Pt < Au). *The S atoms bonded to Au(111) display a unique mobility/reactivity not seen on surfaces of early or late transition metals.* In the next section, we use first-principles DF calculations to examine the adsorption of sulfur on different sites of Au(111) and how the gold−sulfur bonding interactions vary as a function of coverage.

III.2. Bonding of Sulfur to Au(111). The Au(111) surface was represented by a four-layer slab as shown in Figure 7, which was embedded in a three-dimensionally periodic supercell.[45] A vacuum of 12 Å was placed on top of the slab to ensure negligible interactions between periodic images normal to the surface.[22,30] Four-layer slabs are frequently used to model the adsorption of molecules on Au(111).[22,29,30,32] In test calculations (using pseudopotentials), we found similar results for the adsorption of S on four- and six-layer slabs of Au(111). Before building the slab models, we optimized the geometry of bulk gold, obtaining fcc lattice contants (a_o) of 4.155 (PW91 functional), 4.162 (PBE), and 4.171 Å (RPBE) in the pseudopotential calculations. These lattice constants are very close to the experimental value: 4.078 Å.[45b] The adsorbates (S, S_2) were set only on one side of each slab, and their geometry and the geometry of the first two slab layers were completely relaxed in the pseudopotential calculations. For the full-electron calculations, we used the structural geometries obtained using pseudopotentials and the PBE functional.

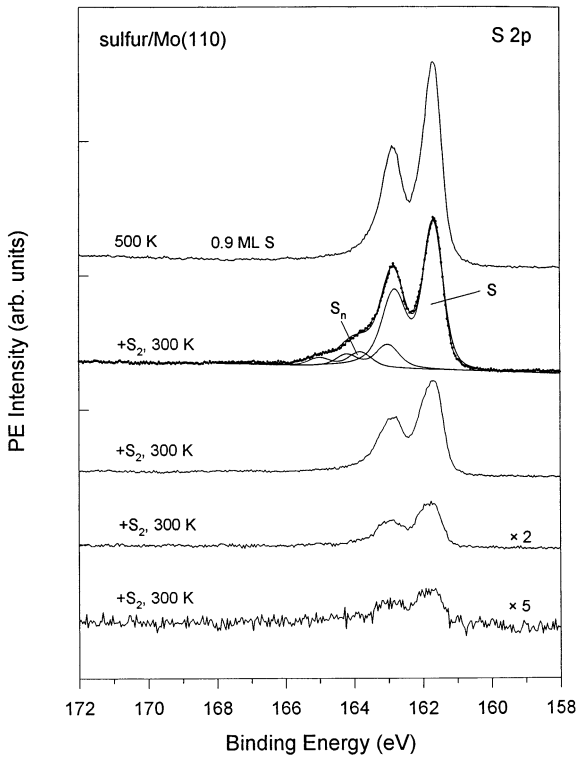

Figure 6. S 2p photoemission spectra for the adsorption of sulfur on Mo(110) at 300 K. In the final step, the sample was heated to 500 K. The sulfur was deposited using a S_2 source, and the coverage is reported with respect to the atomic density of a Mo(110) surface.

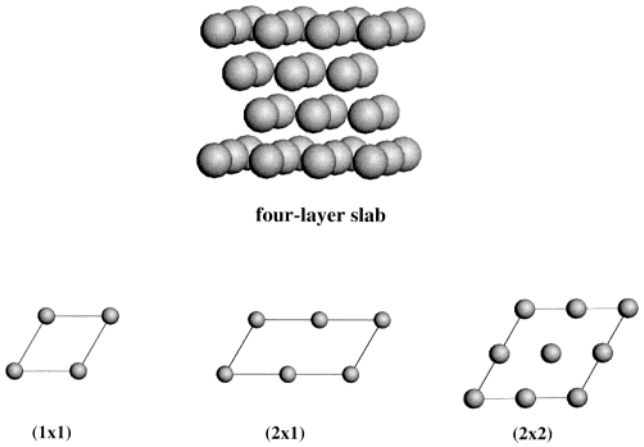

Figure 7. Top: Side view of the four-layer slab used to study the adsorption of S and S_2 on Au(111). Bottom: Top view of the unit cells used for the different coverages of sulfur {1 × 1 or 2 × 1 for 1 ML; 2 × 1 or 2 × 2 for 0.5 ML; 2 × 2 for 0.25 ML} on the gold substrate.

Table 1. Adsorption of Sulfur on Au(111): Pseudopotential DF Calculations

	Au–S distance (Å)			adsorption energy (eV)		
	PW91	PBE	RPBE	PW91	PBE	RPBE
0.25 ML of Sulfur						
(2 × 2) cell, one S atom						
a-top	2.26	2.26	2.27	2.23	2.17	1.92
bridge	2.37	2.36	2.38	3.40	3.31	3.03
hollow hcp	2.41	2.40	2.42	3.66	3.57	3.12
hollow fcc	2.39	2.39	2.39	3.83	3.72	3.31
0.50 ML of Sulfur						
(2 × 1) cell, one S atom						
a-top	2.31	2.32	2.33	2.36	2.26	2.01
bridge	2.39	2.40	2.41	2.75	2.69	2.38
hollow hcp	2.47	2.46	2.47	2.87	2.75	2.46
hollow fcc	2.45	2.44	2.45	2.96	2.83	2.54
(2 × 2) cell, two S atoms or S_2						
hollow fcc, S	2.45	2.43	2.44	5.88	5.64	5.06
brid + a-top S_2	2.46,2.45	2.47,2.46	2.48,2.46	5.99	5.76	5.19
1.0 ML of Sulfur						
(1 × 1) cell, one S atom						
a-top	2.39	2.37	2.40	2.56	2.48	2.09
bridge	2.62	2.61	2.65	2.34	2.26	1.85
hollow hcp	2.72	2.73	2.74	2.32	2.21	1.82
hollow fcc	2.70	2.71	2.73	2.31	2.22	1.81
(2 × 1) cell, two S atoms or S_2						
a-top, S	2.38	2.39	2.40	5.08	4.93	4.14
top + top S_2	2.47	2.46	2.48	6.26	6.06	5.37

Table 1 lists calculated bond distances and adsorption energies for sulfur on Au(111). Using pseudopotentials, we carried out a systematic study with three different exchange-correlation functionals (PW91, PBE, RPBE) and sulfur coverages of 0.25, 0.5, and 1 ML. The switch of exchange-correlation functional did not affect the qualitative trends. As expected,[32,40,57] the RPBE functional gave adsorption energies smaller than those predicted by the PBE and PW91 functionals. The RPBE adsorption energies should be the closest to the experimental values.[32,40] Several key systems were also investigated by means

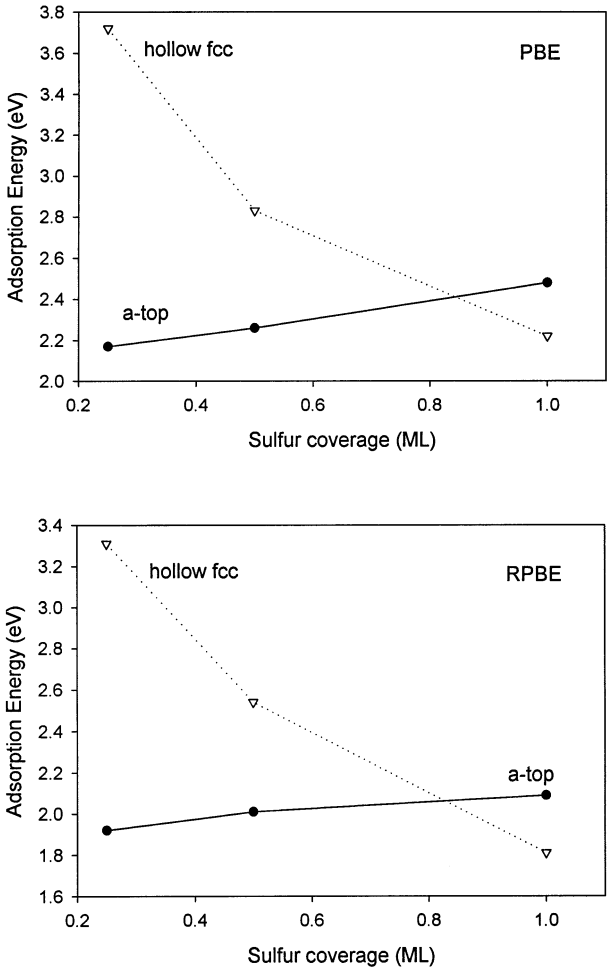

Figure 8. Variation of the S adorption energy on fcc hollow and a-top sites of Au(111) as a function of sulfur coverage. The pseudopotential calculations were performed with either the PBE (top) or the RPBE (bottom) functional.

of full-electron calculations with the PBE functional giving identical trends to those found in the pseudopotential calculations.

For a sulfur coverage of 0.25 ML, the stability of the adsorption sites increases in the following sequence: a-top < bridge < hollow hcp < hollow fcc. In agreement with previous experimental[56,58,59] and theoretical studies[7,32] for the adsorption of S on the ideal (111) face of fcc transition metals, *we find the fcc hollows as the most stable sites for S on Au(111) at low coverages.* The situation drastically changes at medium and large sulfur coverages. As the coverage increases, there is a big drop in the relative stability of the hollow sites (see Figure 8 or Table 1). In fact, for a full layer of atomic S, the a-top site is more stable than any of the hollow sites. At 0.25 ML, the hollow fcc site is more stable than the a-top site by more than 1 eV in the pseudopotential and full-electron calculations. On the other hand, for 1.0 ML, the a-top site becomes more stable than the hollow fcc by 0.1−0.3 eV. As we will see below, these changes in stability are accompanied by variations in the Au(6s,6p)−S(3s,-3p) hybridization.

In the pseudopotential and full-electron calculations, the overall adsorption energy of sulfur substantially decreases with

(57) Rodriguez, J. A.; Ricart, J. M.; Clotet, A.; Illas, F. *J. Chem. Phys.* **2001**, *115*, 454.
(58) Mitchell, K. A. R. *Surf. Sci.* **1985**, *149*, 93.
(59) Wong, P. C.; Zhou, M. Y.; Hui, K. C.; Mitchell, K. A. R. *Surf. Sci.* **1985**, *163*, 172.

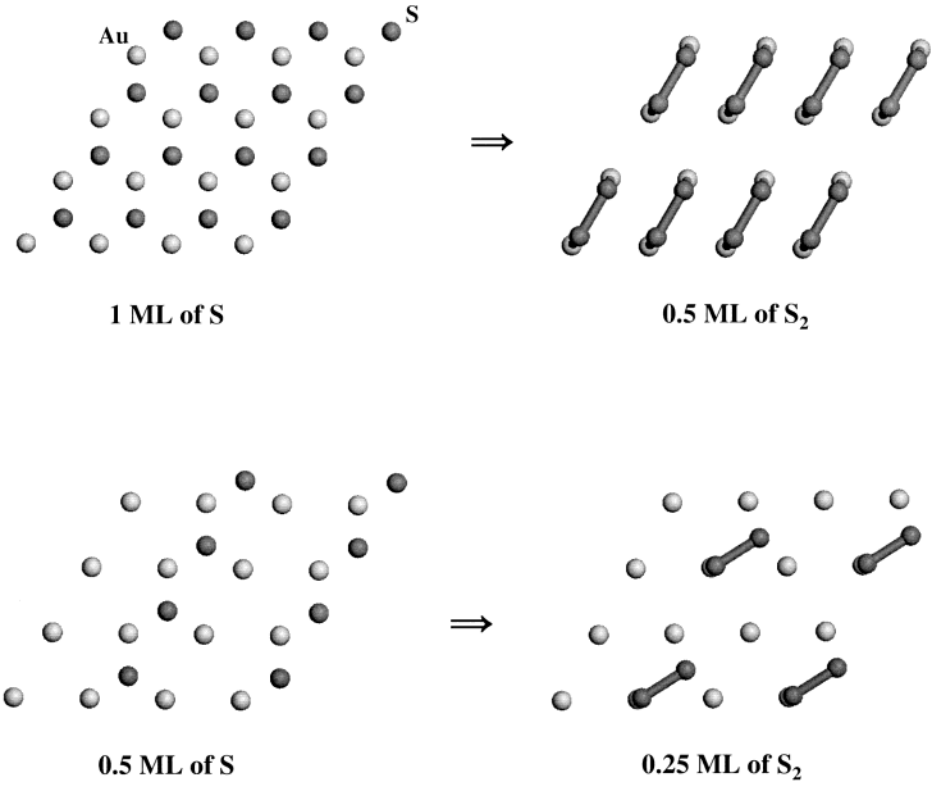

Figure 9. Transformation of S into S_2 on Au(111). Initially, 1 (top) or 0.5 ML (bottom) of S is above fcc hollow sites of the metal substrate. Relaxation of the geometry leads to an overlayer of S_2 molecules. Dark spheres indicate the position of the S atoms.

coverage. The weakening in the Au−S bonds favors S ↔ S interactions, and after full geometry optimization of the systems with 0.5 and 1.0 ML of sulfur, we found that S_2 and not atomic S was the more stable species on the surface. Figure 9 illustrates this in detail for the case of p(1 × 1)- and p(2 × 1)-S/Au(111) surfaces. Initially, the overlayer of atomic S is on the hollow fcc sites, and upon complete relaxation the S atoms move, forming S_2 molecules. In these adsorbed S_2 molecules, the S−S bond distance (1.95−2.0 Å) is somewhat larger than that found for free S_2 (∼1.90 Å). For a p(1 × 1)-S/Au(111) system, the most favorable configuration for atomic S (above a-top sites) is also less stable than a configuration in which the atoms dimerize and the resulting S_2 molecules are parallel to the surface bridging two Au atoms (Au−S−S−Au). The predictions of the DF calculations are consistent with the photoemission results in section III.1, which show a significant amount of S−S bonding when the sulfur coverage on Au(111) is between 0.5 and 1 ML. *Experiment and theory show that the sulfur coverage has a strong impact on the relative strength of the Au−S and S−S interactions*.

For the Au(111) surface covered with a full monolayer of sulfur (one adsorbate atom per surface atom), we performed geometry optimizations with a (2 × 2) cell, and S_2 was more stable than species such as S_3 and S_4. To see the formation of S_n ($n > 2$) aggregates, we have to put more than a monolayer of sulfur on the Au(111) surface. Interestingly, TDS data collected during the heating of a sulfur monolayer show only desorption of S_2, but evolution of S_3 and S_4 is observed during the heating of sulfur multilayers (see section III.1).

At small coverages, S bonds to Mo(110) above quasi-three-fold hollow sites.[60] We examined the adsorption of 0.25 and 1.0 ML of sulfur on Mo(110) using a four-layer slab model

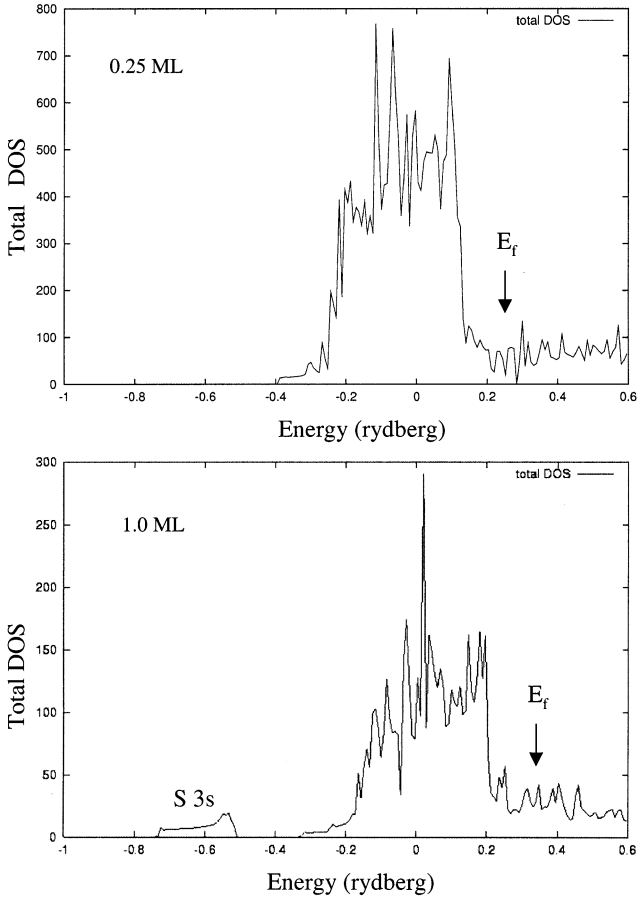

Figure 10. Total DOS plots calculated (full-electron, PBE functional) for 0.25 and 1.0 ML of atomic S on hollow fcc sites of Au(111). The vertical arrows denote the position of the Fermi edge (E_f). 1 Ry = 13.606 eV.

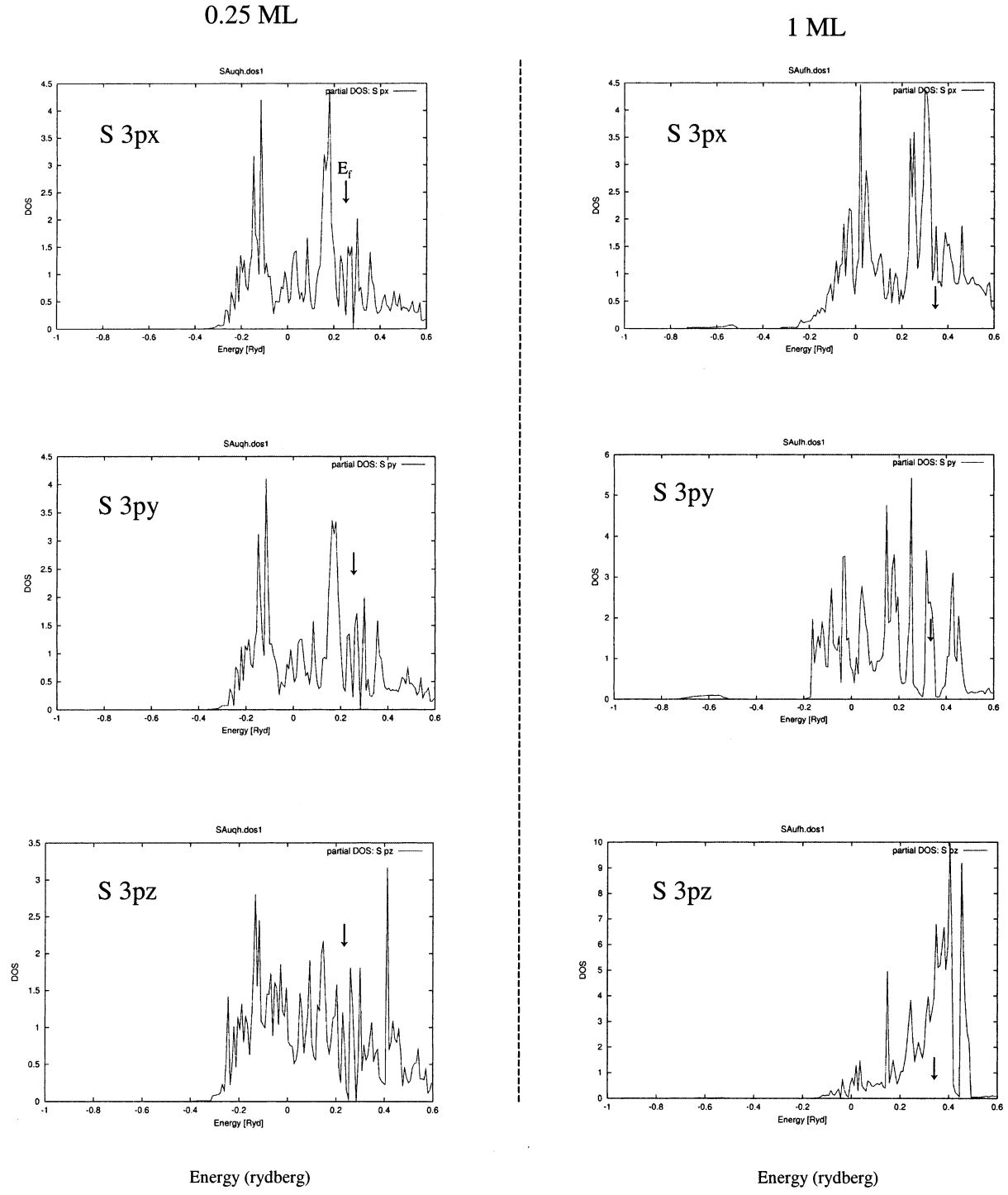

Figure 11. Partial DOS plots for the S 3p states in S/Au(111). Adsorption of S on hollow fcc sites with a coverage of 0.25 (left) or 1.0 ML (right). Full-electron calculations, PBE functional. The vertical arrows denote the position of the Fermi edge (E_f). In our coordinate system, the *z*-axis is normal to the surface. 1 Ry = 13.606 eV.

and first-principles pseudopotential calculations. In general, the adsorption energy of atomic sulfur was 1.8−2.1 times larger than that on Au(111). As in the case of S/Au(111), there was a drop in the adsorption energy of S with coverage for the S/Mo(110) system, but on the molybdenum surface a quasi-three-fold hollow site was always the most favorable adsorption site, and atomic S was more stable than S_2 or S_n aggregates. *These differences highlight how unique and complex the behavior of the sulfur/gold interface can be.* Our experimental and theoretical results suggest that the coverage can play an important role in the structural properties of self-assembled monolayers of thiols grown on gold surfaces.[9,11b] At small gold coverages, the gold substrate can make relatively strong bonds with sulfur, and

(60) (a) Chen, M.; Clark, P. G.; Mueller, T.; Friend, C. M.; Kaxiras, E. *Phys. Rev. B* **1999**, *60*, 11783. (b) Toofan, J.; Tinseth, G. R.; Watson, P. R. *J. Vac. Sci. Technol., A* **1994**, *12*, 2246.

no S−S bonding is expected, in agreement with the predictions of several theoretical studies for the CH_3S/Au(111) system.[22,27,30,32] As the adsorbate coverage increases, there will be a weakening in the strength of the Au−S bonds, which facilitates changes in the adsorption site and could lead to S−S bonding.

The nature of the bond between sulfur and metals is an important subject in catalysis,[1−3,14] electrochemistry,[4−6] interfacial physics,[7,8] and materials science.[9−12] Usually an electronegative element like sulfur[61] is expected to withdraw charge from metal surfaces.[2,14] However, among the transition metals, gold has the highest Pauling electronegativity, very close to that of sulfur (2.58 for S versus 2.54 for Au).[61] In our pseudopotential calculations, we found that the Au−S bond was mainly covalent with small negative charges on adsorbed S and S_2 species. For atomic S, the calculated Mulliken charges varied from ~ -0.2e at $\theta_S = 0.25$ ML to ~ -0.1e at $\theta_S = 0.5$ ML to $\sim$0e at $\theta_S = 1$ ML. *Thus, as the sulfur coverage increases, there is a weakening of the Au−S bonds (Figure 8) and a simultaneous reduction of the Au → S charge transfer*. On adsorbed S_2, the charge (~ -0.05e) was almost zero. At all coverages, we found that S and S_2 species induced a significant decrease in the density of states (DOS) that Au exhibits near the Fermi edge. Previous theoretical studies for the adsorption of S on Pt,[7] Pd,[1,62] and Rh[1,62] also show an adsorbate-induced decrease in the DOS of the metal substrate near the Fermi edge. The decrease in the gold DOS near the Fermi edge should affect the ability of this metal to respond to the presence on adsorbates[1,3c,62] and could play an important role in the poisoning of catalytic and electrocatalytic processes by sulfur.[3,21]

The bond between Au and S was mainly a consequence of a Au(6s,6p)−S(3s,3p) hybridization. The sulfur orbitals involved in the adsorption bond changed with coverage. Figure 10 displays DOS plots obtained in full-electron calculations for 0.25 and 1.0 ML of atomic S on hollow fcc sites of Au(111). The intense features from −0.2 to 0.2 Ry correspond to the Au 5d band, and above these appear S 3p and Au 6s,6p features. For a sulfur coverage of 0.25 ML, the S 3s states are heavily involved in the adsorption bond and strongly hybridize or mix with the S 3p and Au valence states. This is not the case for a sulfur coverage of 1 ML, where a S 3s band is located well below the Au 5d band. *Evidence for a change in S sp hybridization with coverage* is also found in partial DOS plots for the sulfur 3p states shown in Figure 11. The 3p states move from below to above the Fermi edge (vertical arrows in figure) when the sulfur coverages raise from 0.25 to 1.0 ML. This shift is most noticeable in the case of the $3p_z$ states, which are essential for strong bonding interactions between the sulfur overlayer and underlying gold substrate (in our coordinate system the *z*-axis is normal to the surface). Because at high coverage the metal is not able to interact well with all of the adsorbate atoms, there is not need for a substantial sp hybridization in sulfur.

(61) Allred, A. L. *J. Inorg. Nucl. Chem.* **1961**, *17*, 215.
(62) (a) Feibelman, P. J.; Hamann, D. R. *Surf. Sci.* **1985**, *149*, 48. (b) Wilke, S.; Scheffler, M. *Phys. Rev. Lett.* **1996**, *76*, 3380.

IV. Conclusions

Our photoemission and DF results show a complex behavior for the sulfur/Au(111) interface as a function of coverage and temperature. At small sulfur coverages, the adsorption of S on fcc hollow sites of the gold substrate is energetically more favorable than adsorption on bridge or a-top sites. Under these conditions, S behaves as a weak electron acceptor but substantially reduces the DOS that gold exhibits near the Fermi edge. As the sulfur coverage increases, there is a weakening of the Au−S bonds (with a simultaneous reduction in the Au → S charge transfer and a modification in the S sp hybridization) that facilitates changes in adsorption site and eventually leads to S−S bonding. At sulfur coverages above 0.4 ML, S_2 and not atomic S is the more stable species on the gold surface. Formation of S_n ($n > 2$) species occurs at sulfur coverages higher than a monolayer. Very similar trends were observed for the adsorption of sulfur on polycrystalline surfaces of gold. The S atoms bonded to Au(111) display a unique mobility/reactivity not seen on surfaces of early or late transition metals.

Acknowledgment. The research carried out at Brookhaven National Laboratory was financed under contract DE-AC02-98CH10086 with the U.S. Department of Energy (Division of Chemical Sciences). The NSLS is supported by the Divisions of Materials and Chemical Sciences of DOE.

JA021007E